Broadband focused waves with compensated spatial dispersion: transverse versus axial balance

Carlos J. Zapata-Rodríguez and Pedro Andrés
Departamento de Óptica, Universidad de Valencia, 46100 Burjassot, Spain

Gladys Mínguez-Vega and Jesús Lancis
Departamento de Ciencias Experimentales, Universitat Jaume I, 12080 Castellón, Spain

Juan A. Monsoriu
Departamento de Física Aplicada, Universidad Politécnica de Valencia, 46022 Valencia, Spain

Received October 11, 2006; revised January 3, 2007; accepted January 8, 2007;
posted January 10, 2007 (Doc. ID 75854); published March 5, 2007

We determine the constraints an *ABCD* optical system must verify to achieve, at the focal region, broadband waves with compensated spatial dispersion either along the optical axis, called on-axis isodiffracting fields, or in the lateral direction, here named in-plane isodiffracting beams. An optical configuration is identified for generating both types of achromatic broadband focused wave fields. An experimental verification is also provided. © 2007 Optical Society of America

OCIS codes: 050.1970, 220.4830, 320.7080.

Light diffraction and interference are dispersive by nature. When a polychromatic plane wave impinges normally onto a diffracting screen, the redder spectral components are diffracted with higher angles than the bluer components. If diffracted light is gathered by a converging spherical lens, the three-dimensional (3D) focal irradiance distribution suffers from both lateral and axial chromatic dispersion. Compensation of spatial chromatic dispersion effects in broadband focused beams is mandatory in several diffraction-based optical applications. Some arrangements have been proposed to compensate for lateral chromatic deviations. In this respect we point out the implementation of 2D image-forming systems with an achromatic,[1] or even apochromatic,[2] point spread function, and the focusing of temporally incoherent light with a high degree of chromatic correction at the back focal plane.[3] Other chromatically compensated optical configurations were developed for precise ultrashort microprocessing of materials at multiple points by use of grating-based beam splitters[4] and when acousto-optic deflectors of ultrafast laser pulses are used for multiphoton laser-scanning microscopy[5] or micromachining.[6] In general, the above optical systems use a certain combination of refractive elements and high-dispersive components as diffractive lenses and gratings.

Spatial locking of the spectral components at a transverse plane goes with chromatic uncoupling along the optical axis, and then the above setups exhibit limited 3D achromatization capacity. In this paper we determine the *ABCD*-system requirements to achieve either lateral or axial chromatic compensation within a focusing geometry. Next we go one step further and we recognize that the system reported in Ref. 3, which was designed to carry out lateral chromatic compensation, may be adapted, under minor transformations, for spectral correction along the optical axis. Finally, some experimental results are presented to verify the validity of our approach.

Under the paraxial regime, the spectral components of the scalar wave function of a polychromatic field satisfies the free-space wave equation

$$[\nabla_\perp^2 + 2i(\omega/c)\partial_z]U_\omega(\boldsymbol{r}_\perp, z) = 0. \tag{1}$$

In Eq. (1), z represents the axial spatial coordinate along which the optical beam is propagating, $\boldsymbol{r}_\perp$ are transverse coordinates, ω is the angular frequency, and c is the speed of light in vacuum. As usual, we have omitted the term $\exp(i\omega z/c)$. Full chromatic compensation is attained when the 3D complex-amplitude distribution of a given time-harmonic wave field is invariant under a change of frequency. Of course, chromatically independent wave fields propagating in vacuum are not solutions of Eq. (1). In other words, diffraction is a typical dispersive phenomenon. Alternatively, we focus our attention on two types of wave fields. The first one has the spectral dependence

$$U_\omega(\boldsymbol{r}_\perp, z) = S(\omega)U_{\omega_0}(\sqrt{\omega/\omega_0}\boldsymbol{r}_\perp, z), \tag{2}$$

where $S(\omega_0)=1$. It satisfies the paraxial wave equation whether $U_{\omega_0}(\boldsymbol{r}_\perp, z)$ does. The reference frequency ω_0 commonly denotes the carrier frequency of pulsed beams or the peak component of the power spectrum, $|S(\omega)|^2$, for incoherent broadband light. When $r_\perp = 0$, the local spectrum for on-axis points remains invariant, except to a constant. Accordingly, any spectral component of the field shows the same axial pattern. For this reason, such a wave is hereafter called an on-axis isodiffracting (OAID) field, though some authors simply speak of isodiffracting beams.[7,8] Instead, at a fixed z, the transverse pattern at different frequencies is shape invariant but scaled by a spec-

0146-9592/07/070853-3/$15.00

trally discriminating lateral magnification, $\beta_t = \sqrt{\omega_0/\omega}$.

The second type of wave field under inspection is

$$U_\omega(\boldsymbol{r}_\perp, z) = S(\omega) U_{\omega_0}(\boldsymbol{r}_\perp, (\omega_0/\omega) z), \tag{3}$$

which implies that the diffracted field at the reference plane, $z=0$, is invariant on frequency. We name this sort of chromatically balanced field in the lateral direction as in-plane isodiffracting (IPID) beam. In this case, the 3D wave field is affected by a longitudinal magnification, $\beta_l = \omega/\omega_0$. Out-of-plane field patterns are scale invariant at the cost of undergoing a frequency-dependent axial displacement.

Let us next investigate the trade-offs for a diffraction-limited *ABCD* optical system to produce wave fields with invariant chromatic response around the focal volume, as those described above. With this goal in view, we consider that the input complex amplitude emerging from the aperturing screen is denoted by $U_\omega(\boldsymbol{\rho}_\perp)$. If the incident broadband illumination is uniform over the entire input aperture, $U_\omega(\boldsymbol{\rho}_\perp)$ may be separated into two functions. The first denotes the spectral distribution of the incident radiation, $S_0(\omega)$, whereas the second is a function of the spatial coordinates, which is commonly called the pupil function, $P(\boldsymbol{\rho}_\perp)$. Any parabolic phase term accompanying the input complex amplitude is treated within the *ABCD*-matrix computation as a fictitious lens. In this diffraction problem we examine spectrally invariant pupil functions, which hold for purely absorbing diffracting screens.

Furthermore, under the assumption that the output field is localized in the vicinity of focus, we may use the Debye representation. We consider a lens combination of nondispersive objectives and diffractive lenses in a manner such that the focal plane of the optical arrangement is located at the same position for any spectrum. Accordingly, we fix the reference plane, $z=0$, as the Fraunhofer plane of the optical setup. In mathematical terms, we set the matrix element[3] $A(\omega)=0$. In this case, the diffraction integral in the Debye representation is given by[9]

$$U_\omega(\boldsymbol{r}_\perp, z) = \frac{\omega}{i 2\pi c} \frac{1}{B} \int U_\omega(\boldsymbol{\rho}_\perp) \exp\left(-i \frac{\omega}{2c} \frac{z}{B^2} \rho_\perp^2 \right) \times \exp\left(-i \frac{\omega}{c} \frac{1}{B} \boldsymbol{r}_\perp \boldsymbol{\rho}_\perp \right) \mathrm{d}^2 \boldsymbol{\rho}_\perp, \tag{4}$$

where, obviously, the diffracted field $U_\omega(\boldsymbol{r}_\perp, z)$ satisfies the paraxial wave equation (1). Here B represents the corresponding element of the transfer matrix between the input aperture and the reference plane, and, in general, it depends upon frequency.

From Eq. (4) some constraints should be accomplished to meet full chromatic compensation along either the axial, Eq. (2), or the transverse, Eq. (3), direction. On one hand, taking into account the quadratic phase factor inside the integral symbol, it is apparent that a pattern of nonchromatic shape dependence is found at any z-plane of the focal region when $\omega/B^2(\omega)$ is constant. In this case we have an OAID focused field. Interestingly, the on-axis spectrum differs from that of the incident radiation because $S(\omega) = \sqrt{\omega/\omega_0} S_0(\omega)$, assuming $S_0(\omega_0)=1$, which is inferred from combining Eqs. (2) and (4).

Conversely, the diffraction-induced realization of IPID beams, as in Eq. (3), is achieved when the term $\omega/B(\omega)$ is spectrally invariant. In this particular case, the spectral amplitude of the focused field is preserved, i.e., $S(\omega)=S_0(\omega)$. We point out that it is not possible to fulfill frequency invariance for the terms ω/B and ω/B^2 simultaneously. Based on the *ABCD*-matrix approach, this is the key argument by which to recognize that full 3D chromatic compensation in the focal volume is not physically feasible by free-space propagation.

We emphasize that angular dispersion is mandatory for generating OAID and IPID beams via diffraction, which is accomplished by inserting dispersive elements in the *ABCD* optical system. Otherwise, nondispersive arrangements, where $B(\omega)=B(\omega_0)$, give rise to focused waves showing 3D focal patterns that vary with frequency in both the axial and the transverse directions and, as a consequence, the spectra also change locally.[10] In contrast, this sort of wave experiences a characteristic angular spectrum that is independent on ω and, therefore, may be labeled an iso-angular-spectrum (IAS) wave fields. For a review of the above three types of wave fields, see Ref. 11 and references therein.

Let us consider an optical system composed of a nondispersive objective coupled with a pair of kinoform-type diffractive lenses,[3] as depicted in Fig. 1. A first diffractive lens, DL_1, of focal length $Z(\omega) = Z_0 \omega/\omega_0$, where Z_0 denotes the focal length for ω_0, is placed in front of the nondispersive objective, L, at a distance s. A second diffractive lens, DL_2, of focal length Z_0' for ω_0, is located behind L at a distance s'. Under the constraints (1) $s^{-1}+s'^{-1}=f^{-1}$, which is the lens formula for the objective L, of focal length f, and (2) $Z_0' = -(s'/s)^2 Z_0$, the optical arrangement verifies $A(\omega)=0$. Moreover, by inserting an aperturing screen at a distance a from DL_1, the matrix element B is given by

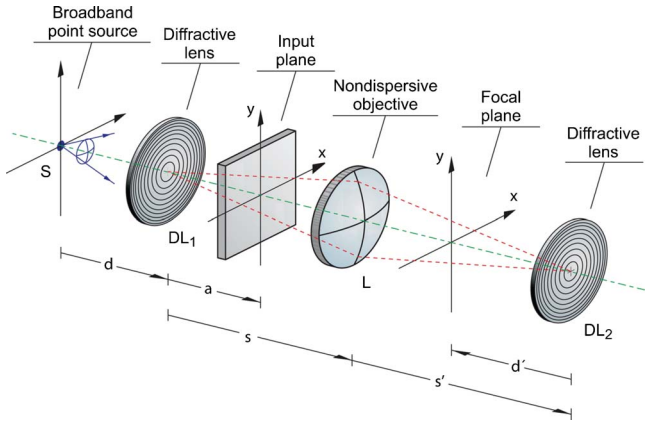

Fig. 1. (Color online) Optical focusing system under consideration.

$$B(\omega) = \frac{f(a+d)}{d-f+s} - \frac{fad\omega_0}{(d-f+s)Z_0\omega}. \quad (5)$$

In Eq. (5) d is the distance from the point source to DL_1. We note that $d>0$ leads to a virtual focal plane, as depicted in Fig. 1.

Unfortunately, neither ω/B nor ω/B^2 is invariant, regardless of the value of the axial parameter a. Alternatively, a less-stringent condition of achromaticity may be required. Concretely, the reference frequency ω_0 is imposed to be stationary for either ω/B or ω/B^2. In Ref. 3 it is demonstrated that, when $a = dZ_0/(2d-Z_0)$, the term $\partial_\omega(\omega/B)$ vanishes for ω_0 and, therefore, the Fraunhofer intensity pattern is achromatic, which was also experimentally verified. Recently, we recognized that, in the Debye approximation, the amplitude distribution is also achromatic.[9] As a consequence, such a scheme produces an achromatic version of IPID focal waves.

On the other hand, to create achromatic OAID fields in the focal volume, we set $\partial_\omega(\omega/B^2)=0$ for ω_0. A solution is found if

$$a = \frac{dZ_0}{3d-Z_0}. \quad (6)$$

Consequently, a simple axial displacement of the diffracting aperture switches the achromatization mode from in-plane to on-axis dispersion compensation. Moreover, the angular dispersion produced by the diffractive lenses may be counterbalanced if $a=0$, which yields an IAS focal wave.

Next we implement the optical device in Fig. 1 to test its axial chromatic compensation capabilities. We choose the focal distances $Z_0=-Z_0'=150$ mm, for $\omega_0=3.34$ PHz, and $f=100$ mm. The axial distances were selected as $d=100$ mm, $s=s'=200$ mm, and, in accordance with Eq. (6), $a=100$ mm. A spherical white-light beam, created from a high-pressure xenon arc lamp, acts as the illumination beam. Finally, a circular aperture of 0.8 mm of radius was located at the input plane. The circular aperture generates several zero-axial irradiance dots for monochromatic illumination. This out-of-focus behavior should be preserved for the generated OAID polychromatic field. The axial irradiance in the region of interest is plotted in Fig. 2(a) for the red, green, and blue (RGB) channels. A picture of the transverse irradiance distribution at the plane marked with an arrow, corresponding to the second zero-axial irradiance point for the green component, is shown in Fig. 3(a). For comparison, Figs. 2(b) and 3(b) illustrate the same experiment when the diffracted field is focused with only the objective L. In the latter case, the zero-axial irradiance dot is clearly blurred.

A second experiment was performed with a zone plate as the input aperture. Here, we emphasize the spectral invariance of the focal-spot axial position observed in the setup depicted in Fig. 1, in contrast to the linearly dispersive focal position commonly achieved under parallel broadband illumination [see Figs. 3(c) and 3(d)].

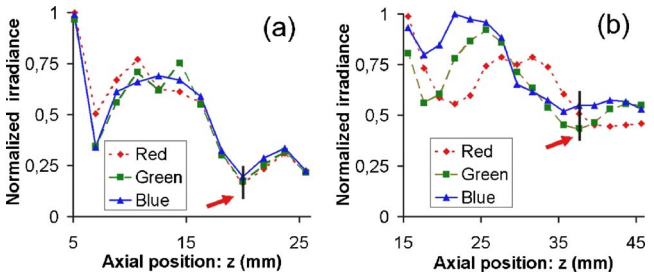

Fig. 2. (Color online) On-axis normalized irradiance for the RGB chromatic components generated by a circular aperture and focused by (a) the achromatic setup in Fig. 1 and (b) an ordinary refractive focusing lens.

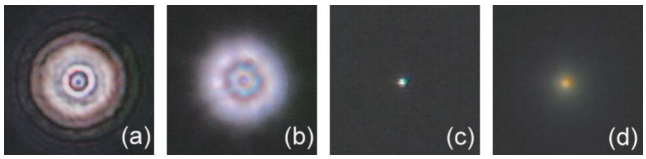

Fig. 3. (Color online) Transverse patterns corresponding to the position of the green component of the second zero-axial irradiance spot produced by a clear circular aperture and the first focus of a zone plate, generated, respectively, by (a) and (c) the setup sketched in Fig. 1 and (b) and (d) without axial achromatic compensation.

This research was funded by the Dirección General de Investigación Científica y Técnica, Spain, and by FEDER, under project FIS2004-02404. C. Zapata-Rodríguez's e-mail address is carlos.zapata@uv.es.

References

1. P. Andrés, V. Climent, J. Lancis, G. Mínguez-Vega, E. Tajahuerce, and A. Lohmann, Opt. Lett. **24**, 1331 (1999).
2. A. Pe'er, D. Wang, A. Lohmann, and A. A. Friesem, Opt. Lett. **25**, 776 (2000).
3. J. Lancis, E. Tajahuerce, P. Andrés, G. Mínguez-Vega, M. Fernández-Alonso, and V. Climent, Opt. Commun. **172**, 153 (1999).
4. J. Amako, K. Nagasaka, and N. Kazuhiro, Opt. Lett. **27**, 969 (2002).
5. S. Q. Zeng, X. Lv, C. Zhan, W. R. Chen, W. H. Xiong, Q. Luo, and S. L. Jacques, Opt. Lett. **31**, 1091 (2006).
6. B. K. A. Ngoi, K. Venkatakrishnan, B. Tan, P. Stanley, and L. E. N. Lim, Opt. Express **9**, 200 (2001).
7. E. Heyman and T. Melamed, IEEE Trans. Antennas Propag. **AP-42**, 518 (1994).
8. M. A. Porras, Phys. Rev. E **58**, 1086 (1998).
9. C. J. Zapata-Rodríguez, J. Opt. Soc. Am. A **24**, 675 (2007).
10. C. J. Zapata-Rodríguez and J. A. Monsoriu, J. Opt. Soc. Am. A **21**, 2418 (2004).
11. C. J. R. Sheppard, J. Opt. Soc. Am. A **18**, 2594 (2001).